

Analysis of Signal to Noise Ratio in Photonic Beamformers

N. M. Froberg, E. I. Ackerman and C. H. Cox III
Photonic Systems, Inc.
900 Middlesex Turnpike, Building 5
Billerica, MA 01821
978-670-4990 x213
nfroberg@photonicsinc.com

Abstract—The goal of this paper^{1,2,3} is to evaluate the impact of photonic beamformers on the amplitude and the signal-to-noise ratio (SNR) of RF signals received by a phased array antenna. To this end, the two-port definitions of RF gain and noise figure are generalized to include multiple-port combining devices such as beamformers. These metrics are then applied to several simple photonic and hybrid RF/photonic beamformer architectures. The gain and noise figure are determined in large part by the components at the photonic interfaces, namely the laser, modulator and photodetector, and therefore all component parameters must be held constant when comparing different beamformer architectures.

As expected, reducing optical loss in the beamformer is essential for achieving high RF gain and SNR at the beamformer output. While the addition of optical amplifiers increases the effective beamformer gain, it also introduces noise which drives up the noise figure. Efficient combining in the beamformer via WDM (wavelength division multiplexing) and/or RF combiners with high coupling efficiency such as Wilkinson combiners can yield a high effective gain without adding additional noise.

TABLE OF CONTENTS

1. INTRODUCTION.....	1
2. BEAMFORMER METRICS.....	2
3. NOISE TERMS IN THE PHOTONIC DOMAIN.....	3
4. GAIN AND NOISE FIGURE CALCULATIONS.....	4
5. RESULTS – SINGLE STAGE BEAMFORMERS	6
6. SYSTEM LEVEL CONSIDERATIONS.....	9
7. CONCLUSIONS.....	9
REFERENCES	11
BIOGRAPHIES	11

1. INTRODUCTION

Photonic beamformers for phased array antennas (PAAs) have long been of interest, due to their inherently wide bandwidth, ability to provide low-loss, dispersion-free time

delays, potential for remote beamforming, and resistance to EMI. Many interesting beamforming architectures have been proposed and demonstrated, ranging from integrated lithium niobate photonic time delay units (TDUs) [1] to broadcast-and-select beamsteering approaches such as the fiber optic Rotman lens [2], to the use of wavelength tunable lasers and fiber optic dispersive delay lines to steer beams [3]. Photonic TDUs using fiber, planar waveguide and free-space micro-optic delay lines have been demonstrated and several types are now commercially available.

Spurred by the deployment of WDM fiber optic networks over the last decade, designers of commercial photonic components have improved their performance significantly, and most components have also come down dramatically in cost. These developments make photonic beamforming a more practical option than it was at its inception in the 1980s. However, beamformers based on RF phase shifters and attenuators at the element level are still able to satisfy the bandwidth demands of most PAA applications more cost-effectively than photonic beamformers. Unless a need develops for ultra-wideband radar systems requiring time delays at the element level, there is still work to be done before photonic beamforming will be able to compete with traditional RF technology.

The deployment of photonic beamformers also hinges on their performance and other benefits that they might bring to a PAA radar system. A key issue for the receive path is whether photonic beamformers can match RF beamformers in SFDR (spur-free dynamic range), limited at the low end by noise and at the high end by distortion. When built with existing COTS components that could feasibly be deployed in practical systems, the photonic links that comprise a photonic beamformer have two-port noise figures in excess of 20 dB, and therefore require LNAs at their inputs to give acceptable SNR at the beamformer output. If the required SNR could be obtained without LNAs in the front end, a common source of failure would be eliminated, distortion would be reduced, and power consumption and thermal signatures at the array would be minimized, resulting in a significant improvement in the PAA system. While the elimination of the LNA is a long-term goal, smaller, nearer-term increases in system SNR would also reduce power consumption and distortion by requiring less gain from the LNA.

¹ 0-7803-9546-8/06/\$20.00© 2006 IEEE

² IEEEAC paper #1067, Version4, Updated Jan 22, 2006

³ Approved for public release 05-MDA-1288 (19 JAN 06)

The most obvious way to improve SNR at the beamformer output is to improve the two-port noise figure of the photonic links; this topic is being addressed by efforts such as DARPA's ULTRA-T/R program [4]. However, the beamformer design also has impact on the output SNR. Because maximizing SNR is a fundamental goal for radar systems, photonic beamformer architectures should be designed to this end.

The goal of this paper¹ is to define metrics for photonic beamformers that can reflect their impact on SNR, and apply them to some simple beamforming architectures in hopes of discovering basic guidelines for beamformer design. Section 2 introduces the generalized definitions for gain and noise figure that have been chosen as appropriate metrics. Section 3 summarizes noise terms generated in the optical domain, with emphasis on noise generated by optical amplifiers. Section 4 describes the calculations and the assumptions made about how noise terms from separate inputs add when combined. Section 5 presents modeling results for some simple beamforming architectures, and Section 6 briefly discusses some system-level considerations. Finally, conclusions are presented in Section 7.

2. BEAMFORMER METRICS

The relationship between SNR of the aggregate signal at the beamformer output (SNR_{out}) and SNR of the received signals at the beamformer input (SNR_{in}) has been studied in the RF domain for active array antennas [5-8]. Lee derived expressions for G/T and noise figure for active arrays, assuming an LNA at every array element and RF combining [5]. This paper applies a similar approach to photonic beamformers, using slightly different metrics that take into account the noise terms generated in the photonic domain. The analysis here is rudimentary compared to the references cited above; future work will refine the analysis and relate it to the previous work.

The standard metrics for quantifying signal strength and SNR in a microwave photonic link (or any two-port device) are gain and noise figure, and these metrics capture the properties of interest in the beamformer: first, the beamformer's effect on signal amplitude, which dictates how much additional gain will be needed after the beamformer, and second, its effect on SNR, which determines the minimum detectable signal and consequently the radar range.

Since these two-port metrics supply exactly the information that is needed, the simplest approach is to extend their definitions from two ports to multiple ports. A beamformer or combiner has multiple inputs and usually a single output;

however, the generalized definitions must also cover beamformers that generate multiple beams.

The proposed definition of *effective beamformer gain*, $G_{RF,eff}(N)$, is:

$$G_{RF,eff}(N) = \frac{S_{RF,out}}{\langle S_{RF,in} \rangle} \quad (1)$$

where $S_{RF,out}$ is the RF power at a single beamformer output with N input signals present, and $\langle S_{RF,in} \rangle$ is the average RF power at each beamformer input. Note that this definition is not consistent with [5-8], which reference the total input power rather than the input power per element.

The proposed definition of *effective noise figure*, $NF_{eff}(N)$, is:

$$NF_{eff}(N) = \frac{SNR_{in}(thermal)}{SNR_{out}} = \frac{N_{RF,out}}{G_{RF,eff}(N) * KTB} \quad (2)$$

where $SNR_{in}(thermal)$ is the average SNR at the beamformer inputs, assuming thermal noise, SNR_{out} is the resulting SNR at a single beamformer output with N input signals present, and $N_{RF,out}$ is the total noise at a single beamformer output with N inputs present. In the case of a beamformer with multiple outputs, these metrics can be calculated for each output, effectively treating the beamformer as if it were multiple beamformers.

Although gain and noise figure are commonly given in dB, note that all equations for gain and noise figure in this paper are in linear units. Also, in the equations above, amplitude variations at the beamformer inputs are lumped into an average value rather than being rigorously accounted for. This first-order approximation is applied throughout the paper, and will be refined in future work.

Figure 1 shows how the effective gain and noise figure metrics would be applied to an RF combiner with N inputs, each having gain G_1 and noise figure NF_1 (using the conventional two-port definitions). Assuming perfect impedance matching, and also assuming that the noise from individual inputs is uncorrelated, the effective noise figure for this general scenario is:

$$NF_{RF,eff}(N) = \frac{1}{G_{RF,eff}} + \frac{NF_1}{N} - \frac{1}{N * G_1} \approx \frac{1}{G_{RF,eff}} + \frac{NF_1}{N} \quad (3)$$

where the first term results from the thermal noise generated by the combiner and the second and third terms result from the uncorrelated noise at the inputs. If the second term dominates, the noise figure after combining is reduced by N relative to the noise figure at the input.

¹Approved for public release 05-MDA-1288 (19 JAN 06)

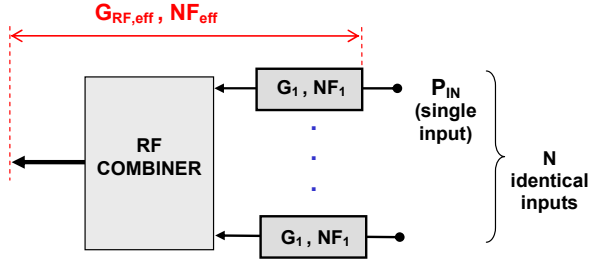


Figure 1. Effective gain and noise figure for an RF combiner with N inputs, each having gain G_1 and noise figure NF_1 .

The effective gain depends on the type of RF combiner used. In this paper¹, an N -way combiner is modeled as a cascade of n 2:1 RF combiners, where the number of stages $n = \log_2(N)$. Ideal impedance matching is also assumed in the combiner cascade; mismatches would result in loss and reflected power that would be dissipated in the combiner network. The least efficient RF combiner is a resistive power combiner, for which $|S_{21}| = 1/2$ and the excess loss per stage is $L_{EX,RC}$. The use of Wilkinson combiners, for which $|S_{21}| = 1/\sqrt{2}$ and the excess loss is $L_{EX,WC}$ per stage, gives a factor of N increase in effective gain over the resistive combiner [9]. The effective gains for these cases are given in equations (4a) and (4b), respectively. A still more efficient way of combining photonic signals in the RF domain is coherent summation of photocurrents, which theoretically gives an N^2 increase in effective gain [10], as in equation (4c), where $L_{EX,CC}$ is the excess loss associated with this process.

$$G_{RF,eff}(N) = G_1 * (L_{EX,RC})^n \quad \text{resistive combiner} \quad (4a)$$

$$G_{RF,eff}(N) = N * G_1 * (L_{EX,WC})^n \quad \text{Wilkinson combiner} \quad (4b)$$

$$G_{RF,eff}(N) = N^2 * G_1 * L_{EX,CC} \quad \text{current combining} \quad (4c)$$

Before applying the generalized definitions of gain and noise figure to photonic links, in Section 3 we will summarize the noise terms generated in the photonic link and provide a brief description of signal-spontaneous beat noise, a dominant noise term that arises when optical amplification is included in the beamformer.

3. NOISE TERMS IN THE PHOTONIC DOMAIN

The basic noise terms in a photonic link – RIN, shot noise and thermal noise – are well understood [11]. RIN, or relative intensity noise, results from intensity fluctuations in the laser output; shot noise results from the randomness in the photon's arrival time. Thermal noise can be generated at the source, the modulator and the detector; the

contribution from a traveling wave modulator is usually small and has been omitted in this analysis. In a photonic link, RIN and/or shot noise typically dominate at high optical power, while thermal noise dominates at low power.

The loss of photonic time delay units (TDUs), variable optical attenuators (VOAs) and combiners used for photonic beamforming can be compensated for by including EDFAs (Erbium-doped fiber amplifiers) or another type of optical amplification in the beamformer. However these amplifiers also add noise to the system and this noise must be taken into account in calculating RF noise figure. In the case of EDFAs, amplified spontaneous emission (ASE) proportional to the EDFA gain beats with the signal and with itself at the photodiode, generating signal-spontaneous beat noise and spontaneous-spontaneous beat noise, respectively. The latter can be filtered for most applications and is negligible for the beamformers analyzed in this paper.

EDFAs are generally characterized by two parameters: optical noise figure and saturated output power. The saturated output power is the maximum optical power that the amplifier can generate. The optical noise figure is defined as the ratio of the (optical) SNR at the EDFA input to the SNR at the EDFA output, assuming that the input SNR is shot-noise-limited. If signal-spontaneous beat noise dominates the output SNR, the EDFA noise figure NF_{EDFA} is given by [12]:

$$NF_{EDFA} = 2 n_{sp} * \frac{G_{EDFA} - 1}{G_{EDFA}} + \frac{1}{G_{EDFA}} \quad (5)$$

where G_{EDFA} is the optical gain of the EDFA and n_{sp} , the spontaneous emission factor, is an intrinsic measure of the noisiness of the EDFA. Equation (5) shows that if $G_{EDFA} \gg 1$, the noise figure is about twice the spontaneous emission factor. EDFAs are often operated in deep saturation, at which point the gain is limited by the saturated output power. The noise figure in deep saturation can be higher than the noise figure in the linear regime, so care must be taken to use the value of noise figure appropriate to the actual operating condition of the amplifier.

Although noise figure is the standard metric for EDFAs, the spontaneous emission factor is a more suitable one as it does not vary with gain. Both the spontaneous emission factor and the saturated output power are functions of the EDFA doping, pump wavelength, and other design parameters. Distortion is not addressed in detail in this paper; however EDFAs have not been found to add distortion to photonic links [13].

Equation (6) gives the expression for the noise current density generated by signal-spontaneous beat noise:

$$i_{s-sp}^2 = 4 r_{det}^2 h \nu n_{sp} P_{opt,in} G_{EDFA} (G_{EDFA} - 1) B \quad (6)$$

¹ Approved for public release 05-MDA-1288 (19 JAN 06)

where r_{det} is the detector responsivity, ν is the optical frequency, B is the RF bandwidth, and $P_{\text{opt, in}}$ is the optical power at the input to the EDFA [12]. This expression is used in the following analysis, assuming typical values for EDFA noise figure and output power. This model illustrates, to first order, how optical amplification affects the RF noise figure of a photonic link (or a beamforming network of photonic links¹).

Figure 2 shows the contributions to noise figure for an optically amplified photonic link as a function of optical loss after the modulator. The noise figure for an unamplified link is shown for comparison. As the link loss increases, addition of an EDFA clearly improves the noise figure. However, signal-spontaneous beat noise replaces shot noise as the dominant noise source, and at very low loss the addition of an EDFA actually degrades the link noise figure as shown in Figure 2.

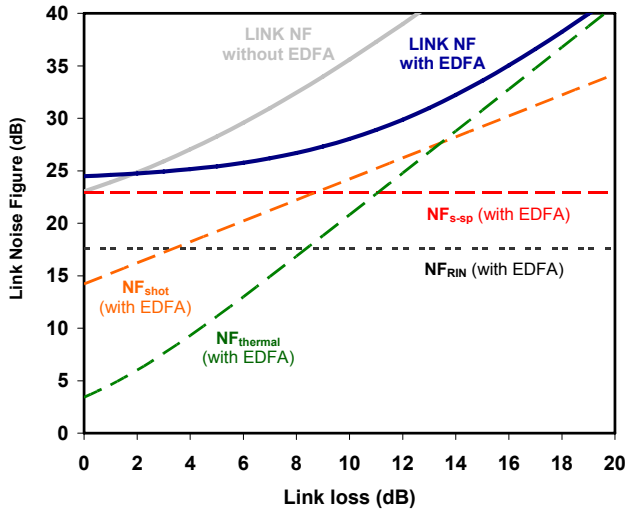


Figure 2. Primary contributions to noise figure as a function of loss in an optical link with and without an EDFA, assuming laser power $P_L = 63\text{mW}$, $RIN = -165\text{ dB/Hz}$, modulator $V_\pi = 1.8\text{ V}$, modulator excess loss = 6.5 dB , detector responsivity = 0.7 A/W , EDFA NF = 5 dB , EDFA output power = 15 dBm . All loss is located at the amplifier output. The noise figure generated by each type of noise (shot, thermal, RIN and signal-spontaneous beat noise) is shown for the case with an EDFA.

Minimizing signal-spontaneous beat noise is clearly essential to minimizing the noise figure of an amplified photonic link. Using equation (6), the noise figure resulting from signal-spontaneous beat noise only in an external modulation link is:

$$NF_{s-sp} = \frac{h\nu}{kT} \left(\frac{V_\pi}{\pi} \right)^2 \frac{4n_{sp}}{R_m P_{\text{opt, in}}} \frac{(G_{\text{EDFA}} - 1)}{G_{\text{EDFA}}} \propto V_\pi^2 \frac{n_{sp}}{P_{\text{opt, in}}} \quad (7)$$

where V_π is the modulator on-off voltage and R_m is the resistive portion of the modulator impedance. Consequently, there are three ways to minimize noise figure when it is dominated by optical amplification:

1. Minimize the modulator V_π .
2. Minimize the spontaneous emission factor n_{sp} of the EDFA (related to the optical noise figure of the amplifier by equation 5).
3. Maximize $P_{\text{opt, in}}$, the input power to the optical amplifier, by maximizing the laser power, minimizing the modulator loss, and placing the amplifier before any sources of loss in the link.

The effect of signal-spontaneous beat noise on beamformer SNR is discussed in the next section.

4. GAIN AND NOISE FIGURE CALCULATIONS

This section describes in detail the calculation of effective gain and noise figure for beamformers. The conditions of the analysis are summarized below:

- *External modulation* – Because photonic beamformers are best suited to applications requiring wide-band, low noise beamforming, the calculations are done for the case of external modulation; specifically, a Mach-Zehnder modulator modulates the RF signal onto a CW light source.
- *No LNAs* – While in a practical system LNAs would be placed before the photonic antenna interface to compensate for beamformer loss, the point of these calculations is to quantify the effect of the beamformer design on SNR and signal strength. Adding an LNA before the beamformer only masks the differences in designs. Therefore, the calculations are done with no amplification before the photonic interface. The effect of adding an LNA to the front end will be discussed later.
- *A separate optical source at each element* – This assumption affects whether or not RIN terms are correlated, as will be discussed later.
- *Matched detectors* – The photodiodes are assumed matched to $50\ \Omega$ (using a $50\ \Omega$ shunt resistor).
- *Room temperature* – The beamformer and photonic antenna interfaces at its inputs are assumed to be at room temperature.
- *Number of inputs $N < 500$* – The analysis is geared towards beamformers having several hundred elements or fewer. The rationale is that, for the foreseeable future, digital processing will be required at the array level to implement adaptive beamforming and other functions. Thus analog beamformers in the system will process relatively small groups of elements, or subarrays, and the output of each analog beamformer

¹ Approved for public release 05-MDA-1288 (19 JAN 06)

will serve as an input to a digital processor. The digital processor can also provide the longest time delays for each element.

Effective gain calculation

The effective gain $G_{RF, \text{eff}}(N)$, and consequently the effective noise figure $NF_{\text{eff}}(N)$, are strong functions of the photonic E/O and O/E interfaces as well as the beamformer architecture. In the case of an all-photonic beamformer (e.g., both time delays and combining are done in the optical domain, and the beamformer output is the output of a photodiode), and assuming that a Mach-Zehnder modulator is used to convert the received RF signal to an optical signal, the effective RF gain is given by equation (8) below:

$$G_{RF, \text{eff}}(N) = \frac{R_{\text{out}} * r_{\text{det}}^2 S_{\text{opt, det}}^2}{\langle S_{RF, \text{in}} \rangle} = \frac{R_m R_{\text{out}} r_{\text{det}}^2 \pi^2 P_{\text{mod, out}}^2}{4 V_\pi^2} G_{\text{opt, eff}}^2 \quad (8)$$

where $S_{\text{opt, det}}$ is the optical signal power at the photodiode, R_{out} is the output resistance (assumed matched to 50 Ω using a shunt resistor), $P_{\text{mod, out}}$ is the average optical power at each modulator output with the modulator biased at quadrature, and $G_{\text{opt, eff}}$ is the effective optical gain. $G_{\text{opt, eff}}$ is defined similarly to $G_{RF, \text{eff}}$ and NF_{eff} as:

$$G_{\text{opt, eff}} = \frac{\langle P_{\text{opt, det}} \rangle}{P_{\text{mod, out}}} \quad (9)$$

where $\langle P_{\text{opt, det}} \rangle$ is the average optical power at the photodiode with all N inputs present. Note that since the beamformer often has net optical loss rather than gain, $G_{\text{opt, eff}}$ is usually (but not always) < 1 ; it was defined as gain to be consistent with the effective RF gain $G_{RF, \text{eff}}$.

Equation (8) shows that the gain of an all-photonic beamformer with external RF-to-optical modulation is almost completely determined by component parameters at the E/O and O/E interfaces, namely the modulator resistance, insertion loss and V_π , the detector responsivity, and the laser power. The only parameter that is determined by the beamformer architecture is the effective optical gain $G_{\text{opt, eff}}$. Equation (8) can be re-written as:

$$G_{RF, \text{eff}}(N) = G_{RF, \text{link}}(\text{zero loss}) * G_{\text{opt, eff}}^2 \quad (10)$$

where $G_{RF, \text{link}}(\text{zero loss})$ is the two-port gain of a photonic link using the same components, with no optical loss between the modulator output and the photodiode. For the external modulation link assumed in this analysis, it is given

by¹:

$$G_{RF, \text{link}}(\text{zero loss}) = \frac{R_m R_{\text{out}} r_{\text{det}}^2 \pi^2 P_{\text{mod, out}}^2}{4 V_\pi^2} \quad (11)$$

Effective noise figure calculation

From equation (2), the effective noise figure at the output of an optical beamformer is:

$$NF_{\text{eff}}(N) = \frac{N_{\text{out}}}{G_{RF, \text{eff}}(N) * kTB} = R_{\text{out}} * \frac{I_{\text{th, det}}^2 + I_{\text{th, N}}^2 + I_{\text{RIN, N}}^2 + I_{\text{shot}}^2 + I_{\text{sig-sp}}^2 + I_{\text{sp-sp}}^2}{G_{RF, \text{eff}}(N) * kTB} \quad (12)$$

where $I_{\text{th, det}}^2$, $I_{\text{th, N}}^2$, $I_{\text{RIN, N}}^2$, I_{shot}^2 , $I_{\text{sig-sp}}^2$, and $I_{\text{sp-sp}}^2$ are the noise current densities for, respectively: thermal noise generated at the photodiode (assumed matched), thermal noise at the N beamformer inputs, total RIN generated by laser sources at the N inputs, shot noise at the photodiode, signal-spontaneous beat noise, and spontaneous-spontaneous beat noise.

In calculating the effective noise figure of the beamformer, some assumptions need to be made about whether various noise terms are correlated or uncorrelated. These are summarized below:

Shot noise, signal-spontaneous beat noise and spontaneous-spontaneous beat noise are functions of the total optical power at the photodiode; e.g., after the optical combiner. Therefore, correlation is not an issue when the combining is done in the optical domain. If the outputs of several photodiodes are combined with an RF coupler, the shot noise and beat noise terms from each individual photodiode are obviously uncorrelated.

RIN from the inputs is assumed uncorrelated, implying that no inputs share a common laser source, therefore:

$$I_{\text{RIN, N}}^2 = N * I_{\text{RIN}}^2 \quad (13)$$

Where I_{RIN}^2 is the average RIN generated by each input.

Thermal noise – Sources of noise generated at the element level are often uncorrelated (for example, noise generated in the LNAs). However, there are also correlated sources of noise in a radar system, such as sky noise. A system-level noise analysis is beyond the scope of this paper; moreover, the definition of effective noise figure assumes that only thermal noise is present at the inputs. The thermal noise at the inputs was assumed correlated for the calculations in the

¹ Approved for public release 05-MDA-1288 (19 JAN 06)

paper, giving the largest possible value of noise current density at the beamformer output:

$$I_{th,N}^2 = N^2 * I_{th,in}^2 \quad (14)$$

where $I_{th,in}^2$ is the average thermal noise current density at each input. The resulting noise figure due to correlated thermal noise only is then:

$$NF_{eff,thermal}(N) = 1 + \frac{1}{G_{RF,eff}} \quad (15)$$

The expression given in equation (3) for effective noise figure in a beamformer using RF combining assumed uncorrelated thermal noise at the inputs. This equation was modified for the case of correlated thermal noise, and is given in equation (16):

$$NF_{eff}(N) = \frac{1}{G_{RF,eff}} + \frac{NF_1 - 1}{N} + 1 - \frac{1}{N * G_1} \quad (16)$$

For the beamformers described in this paper¹, the difference between the two expressions is negligible because the thermal noise term is always a small fraction of the total noise, which is usually dominated by shot noise and/or signal spontaneous beat noise.

To summarize, the dominant noise terms in the photonic domain (shot noise and signal-spontaneous beat noise) are generated at the detector, while RIN originating from the laser at each element is uncorrelated (assuming that each element uses a separate laser).

The noise terms added by the photonic link – shot noise, signal-spontaneous beat noise, and RIN – all produce noise figures proportional to $1/N$, where N is the number of signals present at the inputs. However, the excess loss of a beamformer also tends to increase with the maximum number of elements that it can process. Therefore the performance of a given beamformer design cannot simply be extrapolated using the $1/N$ dependence.

5. RESULTS – SINGLE STAGE BEAMFORMERS

Several variations on single stage photonic beamformers were analyzed using effective gain and noise figure as the key metrics. The reference architectures are shown in Figure 3.

The first beamformer (labeled “a”) is the all-RF case. The second beamformer (“b”) uses photonic TDUs to provide time delays to each received signal, then converts each time-delayed signal back to the RF domain via a

photodetector and combines using an RF power combiner, Wilkinson combiner, hybrid, or the like. The third beamformer (“c”) uses a passive (broadband) photonic combiner, and may or may not include an EDFA at the combiner output before the photodiode. Finally, the fourth beamformer (“d”) uses a WDM multiplexer (MUX) to combine the received signals.

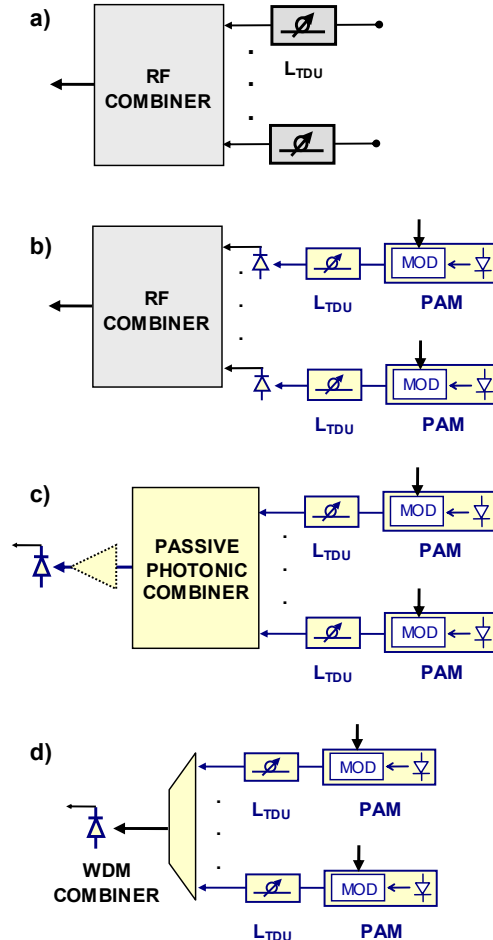


Figure 3. Single-stage beamformer architectures: a) all-RF, b) Photonic TDUs (with optical loss L_{TDU}) with RF combining. The RF signal is converted to optical signal in the photonic antenna module (PAM) via an external modulator (MOD). c) broadband optical combining, optionally with an EDFA at the output, and d) WDM combining, in which wavelengths on separate input fibers are combined onto a single output fiber with much lower insertion loss than a broadband optical combiner.

Contributions to the effective noise figure for cases 3c and 3d are plotted in Figures 4 and 5, respectively, to illustrate some basic trends. Figure 4 shows the noise terms for the photonic beamformer with a passive combiner followed by an EDFA (3c). As expected, signal-spontaneous beat noise dominates the noise figure. Note that the combining of uncorrelated RIN terms reduces the impact of RIN at the

¹ Approved for public release 05-MDA-1288 (19 JAN 06)

beamformer output.

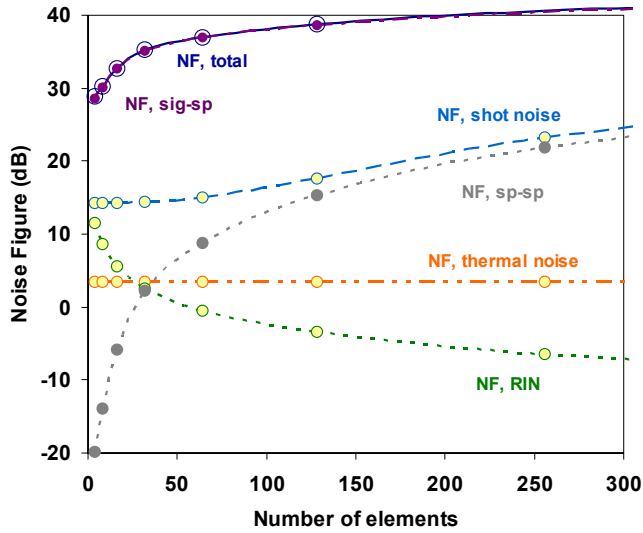


Figure 4. Contributions to noise figure for the beamformer shown in Figure 3c (broadband photonic combiner with EDFA), assuming the same parameters as those used to create Figure 2.

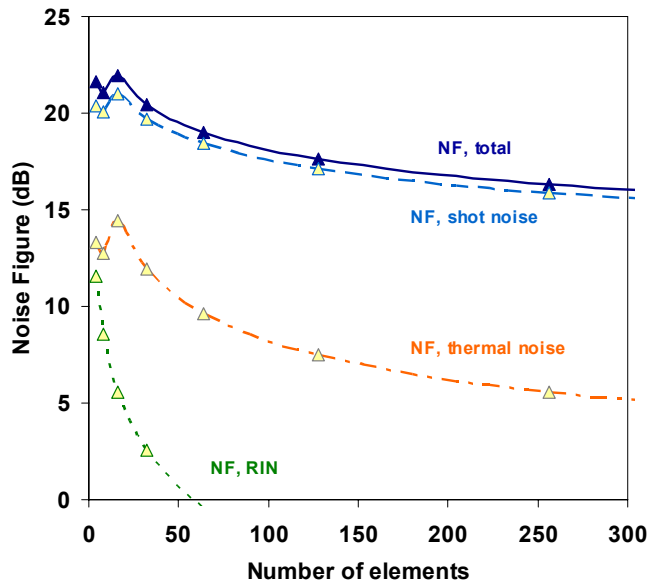


Figure 5. Contributions to noise figure for the beamformer shown in Figure 3d (WDM combining), assuming the same parameters as those used to create Figure 2.

Figure 5 shows the noise contributions for the photonic beamformer with WDM combining (3d) replacing broadband combining (3c). In the broadband optical combiner, the loss experienced by each input signal increases as $1/N$ plus some excess loss. Thus with all N input signals present at the broadband combiner inputs, the net optical power at the combiner output is still less than the signal power at a single input to the combiner¹. On the other hand, a WDM multiplexer combines the power of all

¹ Approved for public release 05-MDA-1288 (19 JAN 06)

N inputs, less some excess loss. Thus the WDM combiner effectively provides gain without adding noise. Shot noise dominates, and the effect of RIN is again minimized by the combining process.

If there is no EDFA in the link, the effective optical gain $G_{opt, eff}$ can be a good predictor of effective noise figure. This is shown in Figure 6. The noise figures for beamformers with photonic combining and no optical amplification (3c without EDFA, and 3d) track the noise figure of a two-port link very well, because in these cases the noise figure is either shot-noise limited or thermal-noise limited, and both are functions of the total photocurrent at the detector.

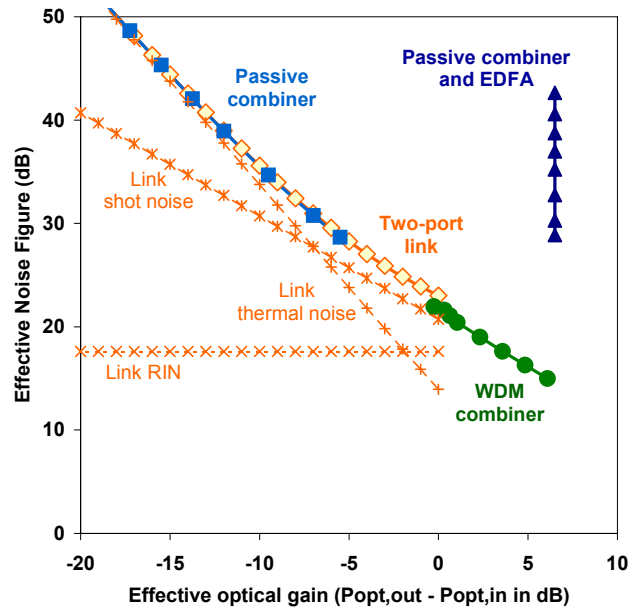


Figure 6. Effective noise figure as a function of effective optical gain for several single stage beamformer architectures, assuming external modulation and the same parameters as in Figure 2. The noise figure is also plotted vs. effective RF gain for a two-port photonic link (diamonds), along with the contribution from each noise term (shot noise, thermal noise and RIN). If there is no optical amplifier in the beamformer and the laser RIN is low, the beamformer noise figure tracks that of the two-port link.

However, the correlation between the beamformer effective noise figure and the effective optical gain is lost when an optical amplifier is added to the beamformer and signal spontaneous beat noise dominates, as is shown by the case of the beamformer with passive combining and an EDFA (triangles in Figure 6). In this case, the gain of the amplifier was adjusted to maintain constant output power, therefore the optical gain remains constant; however, the noise figure increases as the link loss increases, because the additional gain needed to compensate for the loss creates more amplifier noise. The curves would also not track well if the RIN were high enough to dominate the noise figure. In this

case, the link NF would be degraded before the beamformer NF, for which the RIN term is reduced by a factor of N.

Finally, the calculated effective gain and noise figure as a function of the number of inputs N are plotted for each photonic architecture in Figure 7. In an effort to decouple the beamformer performance from that of the photonic antenna interface, the effective beamformer gain and noise figure have been normalized to the corresponding gain and noise figure for a lossless two-port photonic link using the same laser, modulator and detector.

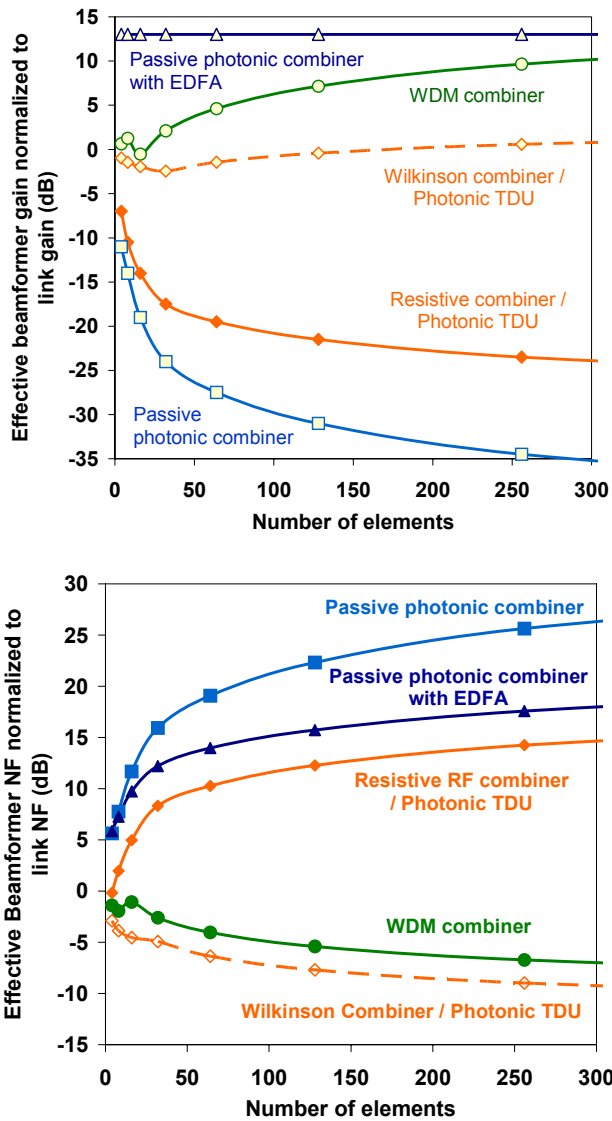


Figure 7. Normalized effective beamformer gain and noise figure vs. number of inputs for several single stage beamformer architectures, assuming the same parameters as in Figure 2. Beamformer gain and noise figure are normalized to two-port gain and noise figure, respectively, for a lossless photonic link. Excess loss assumed per combining stage = 0.5 dB (RF) for RF combiners, 1 dB (optical) for optical combiners; assumed TDU loss = 0.75

dB (optical) per bit¹.

The passive photonic combiner without amplification exhibits the lowest effective gain, and a correspondingly high effective noise figure, in part because every dB of optical loss it adds creates 2 dB of RF loss. Adding an EDFA after the combiner increases the gain dramatically, but the noise figure remains high due to the added signal-spontaneous beat noise.

The combination of photonic TDUs and a resistive RF combiner has less effective loss and therefore better performance than the passive photonic combiner. The same architecture using a Wilkinson combiner with a high coupling ratio (e.g. 3 dB for a 2:1 combiner) provides roughly N times more gain than the resistive combiner and correspondingly lower NF. As noted before, the case where the currents from each photodetector are coherently combined is not shown, but would be expected to have N times more gain than the RF combiner based on Wilkinson combiners.

Of the architectures analyzed, combining with either an RF Wilkinson combiner or a photonic WDM combiner gives the best overall performance, resulting in a lower effective noise figure than that of a two-port photonic link using the same components. In the RF combiner, replacing resistive power combiners with Wilkinson combiners increases the gain by roughly a factor of N; similarly, in the photonic combiner, replacing a broadband coupler with a WDM multiplexer increases the gain by nearly a factor of N².

Table 1 provides a summary of gain and noise figure for each single-stage architecture with 256 inputs, normalized to the gain and noise figure, respectively, of a zero-loss two-port photonic link using the same components at the photonic interfaces.

Table 1. Summary of normalized effective gain and noise figure for single stage beamformer architectures with 256 elements, assuming the same parameters as those used to create Figure 2. The two-port gain and noise figure for a zero-loss photonic link are shown for reference.

Single stage architectures, N = 256	Effective beamformer gain normalized to zero loss link gain (dB)	Effective beamformer NF normalized to zero-loss link NF (dB)
Passive photonic combiner	-35 without EDFA +13 with EDFA	26 without EDFA 18 with EDFA
RF combiner / photonic TDU	-23 resistive -3 Wilkinson	14 resistive -5 directional
WDM combiner	+10	-7
Lossless photonic link	-14	23

¹ Approved for public release 05-MDA-1288 (19 JAN 06)

6. SYSTEM LEVEL CONSIDERATIONS

Note that all of the numbers in Table 1 could be dramatically improved by placing an LNA in front of the photonic interface to the beamformer, as shown in Figure 8. The expression for effective noise figure including the LNA is then:

$$\begin{aligned} NF_{BF,LNA}(N) &= \frac{NF_{LNA} - 1}{N} + \frac{NF_{BF,noLNA} - 1}{G_{LNA}} + 1 \\ &\approx \frac{NF_{BF,noLNA}}{G_{LNA}} + 1 \end{aligned} \quad (17)$$

where $NF_{BF,LNA}$ is the effective noise figure of the beamformer with LNAs at its inputs, $NF_{BF,noLNA}$ is the effective noise figure of the beamformer without LNAs, and G_{LNA} and NF_{LNA} are the gain and noise figure, respectively, of the LNA. To first order, the addition of a front end LNA before the beamformer reduces the effective noise figure by the LNA gain. Since the addition of an LNA masks the effects of different beamformer designs on gain and SNR, it was not appropriate to include them in the architectures being compared in this paper¹.

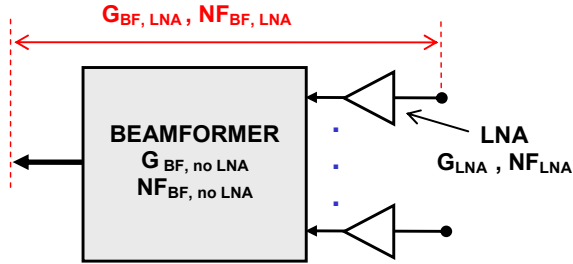


Figure 8. Beamformer with LNAs at each input. The effective noise figure of the beamformer without LNAs is $NF_{BF,noLNA}$, the effective noise figure with LNAs at the beamformer inputs is $NF_{BF,LNA}$, and G_{LNA} and NF_{LNA} are the gain and noise figure of the LNAs, respectively.

The form of equation (17) suggests the use of a slightly different metric for system-level calculations, namely effective noise temperature $T_{BF}(N)$. If the beamformer noise temperature is defined as:

$$T_{BF}(N) = [NF_{BF}(N) - 1] * T_o \quad (18)$$

then equation (17) can be rewritten as:

$$T_{BF,LNA}(N) = \frac{T_{LNA}}{N} + \frac{T_{BF,noLNA}}{G_{LNA}} \quad (19)$$

where $T_{BF,LNA}$ is the effective noise figure of the beamformer with LNAs at its inputs, $T_{BF,noLNA}$ is the effective noise figure of the beamformer without LNAs, and T_{LNA} is the noise temperature of the LNA. Application of this metric in standard radar calculations will be the subject of future work.

7. CONCLUSIONS

In conclusion, the generalized definitions of gain and noise figure presented in this paper are applicable to devices with multiple ports, and can be used to evaluate how beamformer design affects the SNR and signal strength at its outputs. It is important to note that the properties of the components comprising the beginning and end of the photonic link – i.e., the laser, modulator and detector – largely determine the gain and noise figure at the beamformer output, so the same values must be assumed in comparing different beamformer architectures.

Some basic conclusions and observations about the effective beamformer gain and noise figure are summarized below.

- *Effective gain* – As shown in equation (10), the RF gain $G_{RF,eff}$ of the beamformer is:
 - Directly proportional to $G_{RF,link}$, the RF gain of a lossless two-port photonic link using the same photonic E/O and O/E components.
 - Proportional to the square of the optical gain, $G_{opt,eff}$, which is determined by the beamformer design and component loss.
- *Effective noise figure and noise temperature*
 - The effective RF noise figure NF_{eff} , defined as the ratio of the thermal-noise-limited SNR at each beamformer input to the SNR at the beamformer output, is also a useful metric for beamformer performance. The effective noise temperature T_{BF} for the beamformer can be derived from NF_{BF} using the standard relationship given in equation (18).
 - For photonic beamformers without optical amplification, the noise figure is dominated by shot noise in the high-power regime and thermal noise in the low-power regime, and generally tracks the noise figure of a low-RIN photonic link with the same photonic interfaces ($G_{RF,link}$) and effective optical loss ($G_{opt,eff}$).
- *Overall performance of photonic beamformers:*

¹ Approved for public release 05-MDA-1288 (19 JAN 06)

- Optical amplifiers such as EDFAs can increase the gain of a photonic beamformer dramatically, but also add a signal-spontaneous beat noise term that tends to dominate the beamformer noise figure.
 - Efficient combining in the beamformer (via WDM-based photonic combining, RF couplers with high coupling efficiency such as Wilkinson combiners, or possibly coherent current combining) can increase the effective beamformer gain without adding additional noise.
- *Comparison of photonic and hybrid RF/photonic beamformers:*
 - RF and photonic combiners exhibit the same $1/N$ reduction in noise figure at the combiner output. In other words, the noise figure with only one input signal present is roughly N times larger than the effective noise figure with all N inputs present. However, the excess optical loss of the beamformer also increases with the number of inputs.
 - A beamformer with photonic TDUs and RF combining at the output has better performance than an all-photonic beamformer using broadband optical combiners. This is because even resistive RF power combiners introduce less loss to the beamformer than star-type broadband optical combiners (e.g., fused fiber).

Clearly, the reduction of SNR in radar systems using photonic subsystems hinges on the development of high performance photonic components for the E/O and O/E interfaces. However, efficient beamformer design is also required to optimize SNR, and should be a primary goal.

Future work

A key goal for future work is to validate the equations presented in this paper with experimental data. Data on SNR at the beamformer output and inputs will be collected in an upcoming range test of a photonic beamformer.

A second goal is to apply the beamformer metrics proposed in this paper to system-level calculations of signal to noise ratio and other key metrics for practical radar systems. In particular, the effective beamformer gain, noise figure and noise temperature must be related to G/T_s , the standard metric for receive arrays [14], which has been used in the previous work on beamformer SNR. Finally, the metrics proposed here are for the receive path of a phased array antenna; similar metrics must be defined for the transmit path.

Acknowledgments

This material is based upon work supported by MDA under NSWCCD Contract No. N00178-03-C-3110 and MDA Contract No. HQ0006-05-C-7229¹. The views, opinions, and findings contained in this report are those of the author(s) and should not be construed as an official Department of Defense position, policy, or decision, unless so designated by other official documentation.

10 _____

¹ Approved for public release 05-MDA-1288 (19 JAN 06)

REFERENCES

- [1] R. Soref, "Programmable time-delay devices," *Appl. Opt.*, vol. 23, pp. 3736-3737, October 1984.
- [2] R. Sparks, et al., "Eight beam prototype fiber optic Rotman lens," *Proc. IEEE Top. Meeting on Microwave Photonics*, November 1999.
- [3] R. Esman, et al., "Microwave true time-delay modulator using fibre-optic dispersion," *Electron. Lett.*, vol. 28, p. 1905, September 1992.
- [4] E. Ackerman et al., "Low noise figure, wide bandwidth analog optical link", *Proc. IEEE International Topical Meeting on Microwave Photonics*, October, 2005.
- [5] J. J. Lee, "G/T and noise figure of active array antennas," *IEEE Trans. Antennas Propagat.*, vol. 41, p. 241, February, 1993.
- [6] A. K. Agrawal and E. L. Holzman, "Beamformer architectures for active phased-array antennas," *IEEE Trans. Antennas Propagat.*, vol. 47, p. 432, March, 1999.
- [7] U. R. Kraft et al., "Gain and G/T of multielement receive antennas with active beamforming networks," *IEEE Trans. Antennas Propagat.*, vol. 48, p. 1818, December, 2000.
- [8] R. V. Gatti et al., "Computation of gain, noise figure and third order intercept of active array antennas," *IEEE Trans. Antennas Propagat.*, vol. 52, p. 3139, November, 2004.
- [9] David M. Pozar, *Microwave Engineering*, third edition, John Wiley & Sons, 2005.
- [10] J.G. Ho et al., "Wideband coherent combining of photonic RF signals with photodiode array," *GOMAC Tech* 2004, March 15-18, 2004.
- [11] C. Cox, *Analog Optical Links: Theory and Practice*, New York: Cambridge University Press, 2004.
- [12] D. Derickson, editor, *Fiber optic test and measurement*, Prentice Hall PTR, 1998.
- [13] L. Kazovsky et. al., "Dynamic range of analog optical links: do optical amplifiers help?," in *IEEE LEOS Summer Topical Meeting RF Optoelectron. Tech. Dig.* Keystone, CO, Aug. 9-11, 1995, pp. 29-30.
- [14] R. J. Mailloux, *Phased Array Antenna Handbook*, Boston: Artech House, 1993.

BIOGRAPHIES



Nan Moore Froberg holds a BSE degree from Princeton University and the MSEE and PhD degrees from Columbia University. She has over twelve years of experience in the field of fiber optic communications and over 20 years in the general field of optics. She has worked in both product development and research environments, including AT&T Bell Laboratories, Lucent Technologies, and MIT Lincoln Laboratory. Her background and interests include many topics in analog and digital fiber optic transmission, including microwave photonics, WDM technology, optical networking, and transport. She has authored or co-authored over 30 technical papers and holds two patents.



Edward I. Ackerman received his B.S. degree in electrical engineering from Lafayette College in 1987 and his M.S. and Ph.D. degrees in electrical engineering from Drexel University in 1989 and 1994, respectively. He has worked in the area of microwave photonics at Martin Marietta and MIT Lincoln Laboratory, where he developed high-performance analog photonic links for microwave communications and antenna remoting applications. During this time he and Dr. Cox achieved the lowest noise figure ever demonstrated for an amplifierless analog optical link (2.5 dB at 130 MHz). While at Lincoln Laboratory he also developed and patented a novel linearization technique to enable improved analog optical link dynamic range across broad bandwidths and at higher frequencies than other linearization techniques currently allow. Currently he is Vice President of Research and Development for Photonic Systems, Inc. of Billerica, Massachusetts. He has co-edited a book and has authored or co-authored three book chapters as well as more than fifty technical papers on the subject of analog photonic subsystem performance modeling and optimization.



Charles H. Cox III ScD, is one of the pioneers of the field that is now generally referred to as analog or RF photonics. In recognition of this work he was elected a Fellow of the IEEE for his contributions to the analysis, design and implementation of analog optical links. Dr. Cox is President and CEO of Photonic Systems Inc., located in Billerica MA, which he founded in 1998 to provide expert consulting services in fiber-optic system design options and to develop low-cost, high-performance fiber-optic links for government and commercial applications. Prior to founding Photonic

Systems Inc., Dr. Cox was on the research staff at MIT and at Lincoln Laboratory in Applied Physics and Applied Photonics groups. Dr. Cox received his ScD from MIT in 1979 and his Masters (1972) and Bachelor's (1970) degrees from the University of Pennsylvania. He holds six US patents, has given 45 invited talks on photonics and has published over 70 papers on his research in the field of photonics. He has written a textbook titled *Analog Optical Links*, which was published in 2004, as well as two book chapters.

